Proceedings of the International Congress on Ultrasonics, Vienna, April 9-13, 2007, Paper ID 1227, Session R25: Transducer modeling and metrology
doi:10.3728/ICUltrasonics.2007.Vienna.1227_filoux

Combined pseudospectral and finite-difference time-domain methods for ultrasonic transducers modeling

Erwan Filoux, Franck Levassort, Samuel Callé, Pierre Maréchal, Marc Lethiecq

François-Rabelais University of Tours, Laboratoire Ultrasons Signaux et Instrumentation,
10 Boulevard Tonnellé, BP3223, 37032 Tours Cedex 1, France, filoux_e@med.univ-tours.fr

Abstract: Pseudospectral methods are widespread techniques used in electromagnetics and geophysics to model wave propagation in fairly inhomogeneous media. Stability and high accuracy can be achieved from as few as two points per wavelength. A 2D pseudospectral time-domain (PSTD) algorithm was previously developed to simulate the transmit radiation pattern in water of an ultrasonic transducer using the front face pressure as input. Here, this algorithm is improved by taking into account the piezoelectric effect (with mechanical losses) in the active element of the transducer. For this, the PSTD algorithm is combined with a finite-difference time-domain (FDTD) method. From the piezoelectricity constitutive equations under quasi-static approximation, stress and velocity variables are calculated with the PSTD method. Since Poisson equation for the electrical potential is not time dependent, this variable is obtained from the FDTD method. Two different configurations have been investigated. In each case, the piezoelectric element is a PZT plate resonator with a 50 MHz thickness resonant frequency. The first one is composed of the piezoelectric element alone immersed in water. For the second one, a backing and a matching layer are added. Continuity of the electrical field is imposed at the borders of the piezoelectric material and perfectly matched layers (PML) are developed to avoid artifacts from waves reflected on the grid sides. The main characteristic values (displacement, stress and electrical potential) are calculated and are found to be in good agreement with those obtained using a finite element method (ATILA®).

Key words: pseudospectral time-domain (PSTD) method; finite-difference time-domain (FDTD) method; piezoelectricity; transducer modeling.

A. Introduction

The pseudospectral (PS) and finite-difference (FD) methods are widespread techniques used for the simulation of waves propagating in fairly inhomogeneous media [1]. The PS method consists in calculating the derivatives of a variable in the Fourier domain, and requires as few as 2 nodes per minimum wavelength to provide exact solutions [2]. That is why a PS algorithm was previously implemented to model acoustic waves propagation in water. It was combined to a Perfectly Matched Layer (PML) condition at the borders of the computational domain to avoid the incident waves to be reflected and counter the wrap-around effect from the FFT [3]. The algorithm was completed by the simulation of the electrical excitation in order to simulate both the piezoelectric transducer vibration and the resulting wave propagation in the surrounding media, while keeping the different advantages described above. To compute the electric field, quasistatic approximation is assumed, which leads to the resolution of a time independent equation with a second order derivative. As the PS method is not adapted to this kind of operation, we use the FD method to calculate the electric field generated in the piezoelectric media. This method is efficient to model piezoelectric elements with various geometries and materials [4], which is interesting for the simulation of transducers with different structures and excitation sources, but is more limited than the PS method by numerical dispersion. That is why the propagation of acoustic waves over large distances is simulated by the PS method, so that the advantages of both methods are retained.

In the following part we will briefly describe the basis of the theory with the governing equations, including mechanical losses, and the main steps of this hybrid FD-PSTD algorithm. Then we will present the results obtained with this method for the simulation of a two-dimensional piezoelectric element vibrating alone in water and with a configuration closer to that of a real transducer (backing and front matching layer). To validate the FD-PSTD method these results are compared to those obtained with the ATILA finite element (FE) software [5].

B. Model description

B.1. Governing equations

The modeling of piezoelectric vibration and of the acoustic waves propagating in the entire structure of the transducer is based on mechanical and electromagnetic equations. Using Einstein's convention for repeated indices, the propagation of the acoustic waves is described by the following equations [6]:

$$\frac{\partial v_i}{\partial t} = \frac{1}{\rho} \cdot \frac{\partial T_{ij}}{\partial x_j}, \tag{1}$$

$$\frac{\partial T_{ij}}{\partial t} = c^E_{ijkl} \cdot \frac{\partial v_k}{\partial x_l} \cdot \tag{2}$$

The vibration of the piezoelectric element excited by an electrical source is governed by the piezoelectric constitutive equations, associated to Maxwell's relations, which leads to the following system:

doi:10.3728/ICUltrasonics.2007.Vienna.1227_filoux

$$\frac{\partial T_{jk}}{\partial t} = c^E_{jklm} \cdot \frac{\partial v_l}{\partial x_m} - e_{ijk} \cdot \frac{\partial E_i}{\partial t}, \quad (3)$$

$$\frac{\partial D_i}{\partial t} = \varepsilon^S_{ij} \cdot \frac{\partial E_j}{\partial t} + e_{ilm} \cdot \frac{\partial v_l}{\partial x_m}, \quad (4)$$

where $\boldsymbol{v}$ is the particle velocity tensor, $\boldsymbol{T}$ is the stress tensor, $\boldsymbol{D}$ is the electric displacement vector, $\boldsymbol{E}$ is the electric field vector, ρ is the material density, $\boldsymbol{c}^E$ is the stiffened stiffness tensor, $\boldsymbol{e}$ is the piezoelectric tensor and $\boldsymbol{\varepsilon}^S$ is the dielectric permittivity tensor. The losses in the materials are limited to the mechanical ones, the other losses being considered negligible. In the harmonic domain these losses are introduced through imaginary parts of the coefficients of the stiffness tensor:

$$c^E_{ij} = c^E_{ij}'.(1 + j.\alpha'.\omega),$$

with α' the coefficient of a quadratic frequency-dependent attenuation in materials. Equation (3) is then modified and becomes in the temporal domain:

$$\frac{\partial T_{jk}}{\partial t} = c^E_{jklm}'.\left[\frac{\partial v_l}{\partial x_m} + \frac{\alpha'}{\rho} \cdot \frac{\partial}{\partial x_m}\left(\frac{\partial T_{lp}}{\partial x_p}\right)\right] - e_{ijk} \cdot \frac{\partial E_i}{\partial t}. \quad (5)$$

As usual the evolution of the electromagnetic field is considered instantaneous compared to the propagation of mechanical waves. Thus, the quasistatic approximation is used and the description of the electromagnetic field is reduced to the local Gauss relation:

$$div\ \boldsymbol{D} = \rho_e. \quad (6)$$

As there is no free charge inside the piezoelectric element ($\rho_e = 0$), the combination of (4) and (6) leads to a direct relation between displacements and potentials:

$$\frac{\partial}{\partial x_i}\left(\varepsilon^S_{ij} \cdot \frac{\partial \dot{\phi}}{\partial x_j}\right) = \frac{\partial}{\partial x_i}\left(e_{ilm} \cdot \frac{\partial v_l}{\partial x_m}\right), \quad (7)$$

where ϕ is the electrical potential and $\dot{\phi} = \partial\phi / \partial t$. Equations (1), (5) and (7) form a system governing the generation and the propagation of acoustic waves in a piezoelectric media.

B.2. Steps of the algorithm

The calculation is performed in three main steps. The first step (Fig. 1) consists in calculating the temporal derivatives of stress through (5) from the electric field and the acoustic velocity known at $t = n$. This electric field is initialized inside the piezoelectric material by the initial electrical source conditions. To obtain the stress field $\boldsymbol{T}$ at $t = n + \Delta t/2$, the derivatives of stress are integrated using the fourth order coefficients of Adams-Bashforth's (AB) relationship for time-staggered grids [7]:

$$y(t + \Delta t) = y(t) + \frac{\Delta t}{24} \cdot \left[26 \cdot \frac{\partial y}{\partial t}\left(t + \frac{\Delta t}{2}\right) - 5 \cdot \frac{\partial y}{\partial t}\left(t - \frac{\Delta t}{2}\right) + 4 \cdot \frac{\partial y}{\partial t}\left(t - \frac{3\Delta t}{2}\right) - \frac{\partial y}{\partial t}\left(t - \frac{5\Delta t}{2}\right)\right],$$

where Δt is the temporal increment. The use of time-staggered grids enhances the temporal resolution of the model.

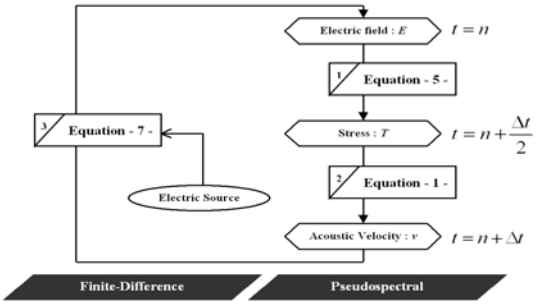

Fig.1. Scheme of the FD-PSTD algorithm.

Then, as a second step, the temporal derivatives of acoustic velocity are calculated by solving (1), and another integration of AB gives the new acoustic velocity field $\boldsymbol{v}$ at $t = n + \Delta t$. These two first steps are solved using the PS method, which consists in calculating the spatial derivatives in the Fourier domain [8]. To obtain, for instance, the first derivative of *Tij* along *xj* axis in the time domain, we perform the following operations:

$$\frac{\partial T_{ij}}{\partial x_j} = FFT^{-1}\left[(-j.k_j).FFT(T_{ij})\right],$$

where the wave number *kj* is the vector:

$$\left(0 \quad \frac{1}{N} \quad \frac{1}{2} \quad \cdots \quad \frac{1}{2} - \frac{1}{N} \quad -\frac{1}{2} \quad \cdots \quad -\frac{1}{N}\right) \cdot j\frac{2\pi}{\Delta x_j},$$

with N the number of nodes along *xj* axis on the grid of *Tij*. Due to the use of FFT operations, these steps require a smooth evolution of the variables in time and space.

The third step consists in solving (7) to calculate the electrical potentials inside the piezoelectric material. In our Cartesian coordinates (defined, for instance, by *x1* and *x3* axes) this equation can be expressed:

$$\varepsilon^S_{11} \cdot \frac{\partial^2 \dot{\phi}}{\partial x_1^2} + \varepsilon^S_{33} \cdot \frac{\partial^2 \dot{\phi}}{\partial x_3^2} + \frac{\partial \varepsilon^S_{11}}{\partial x_1} \cdot \frac{\partial \dot{\phi}}{\partial x_1} + \frac{\partial \varepsilon^S_{33}}{\partial x_3} \cdot \frac{\partial \dot{\phi}}{\partial x_3} = \frac{\partial}{\partial x_1}\left[e_{15} \cdot \left(\frac{\partial v_3}{\partial x_1} + \frac{\partial v_1}{\partial x_3}\right)\right] + \frac{\partial}{\partial x_3}\left[e_{31} \cdot \frac{\partial v_1}{\partial x_1} + e_{33} \cdot \frac{\partial v_3}{\partial x_3}\right],$$

with $\dot{\phi}$ the unknown variable which has to be determined. The second part of the equation is calculated during the previous steps of the algorithm, and will be called *Rj,k*. As this equation is not time dependent it can not be solved using the PS method. That is why a FD representation is used, and it leads to a new discretized expression of the equation:

$$\left(\frac{\tilde{\varepsilon}^1_{11}}{\Delta x_1^2} - \frac{\Delta \varepsilon_{11}^1}{2.\Delta x_1}\right)_{j,k} \cdot \dot{\phi}_{j-1,k} + \left(\frac{\tilde{\varepsilon}^1_{11}}{\Delta x_1^2} + \frac{\Delta \varepsilon_{11}^1}{2.\Delta x_1}\right)_{j,k} \cdot \dot{\phi}_{j+1,k} + \left(\frac{\tilde{\varepsilon}^3_{33}}{\Delta x_3^2} - \frac{\Delta \varepsilon_{33}^3}{2.\Delta x_3}\right)_{j,k} \cdot \dot{\phi}_{j,k-1} + \left(\frac{\tilde{\varepsilon}^3_{33}}{\Delta x_3^2} - \frac{\Delta \varepsilon_{33}^3}{2.\Delta x_3}\right)_{j,k} \cdot \dot{\phi}_{j,k+1} - 2 \cdot \left(\frac{\tilde{\varepsilon}^1_{11}}{\Delta x_1^2} + \frac{\tilde{\varepsilon}^3_{33}}{\Delta x_3^2}\right)_{j,k} \cdot \dot{\phi}_{j,k} = R_{j,k}, \quad (8)$$

with:

$\dot{\phi}_{j,k}$ the temporal derivative of ϕ at node (j, k),

Δx_i the space increment along x_i axis,

$\tilde{\varepsilon}^i_{pq}$ the average value of ε_{pq} along x_i axis,

$\Delta \varepsilon_{pq}^{\ i}$ the derivative of ε_{pq} with respect to x_i axis.

doi:10.3728/ICUltrasonics.2007.Vienna.1227_filoux

As this equation must be solved at each node (j, k) of the grid defined by the unknown potentials, we obtain at each time step a system of linear equations which can be written:

$$\boldsymbol{Q} \,.\, \boldsymbol{X} = \boldsymbol{R} \,,$$

with $\boldsymbol{Q}$ a block tri-diagonal matrix that has to be inverted, $\boldsymbol{X}=\left(\phi_{j,k}\right)_{j,k}$ the unknown vector and $\boldsymbol{R}=\left(R_{j,k}\right)_{j,k}$. When vector $\boldsymbol{X}$ is calculated, the electric field can be easily determined and an other iteration of the algorithm can start.

C. Results

C.1. Piezoelectric element in water

The numerical results of the FD-PSTD method are compared to those of the ATILA® FE software. In order to validate our method the first simulation is performed using the simple two-dimensional model of a thin piezoelectric plate with a half-wavelength thickness, covered on both sides with electrodes excited by a 50 MHz sinusoidal electric signal during half a period. The piezoelectric element is a PZT resonator (Ferroperm Piezoceramics Pz27) polarized in the *x3* direction with a 50 MHz thickness resonant frequency. As the piezoelectric resonator is modeled in the plane containing *x1* and *x3* axes, its characteristics of interest are summarized in Table 1.

Table 1. Coefficients of the stiffened stiffness (10^{10} N/m²), dielectric permittivity and piezoelectric (C/m²) tensors of Pz27.

c_{11}^E	c_{13}^E	c_{33}^E	c_{44}^E	$\varepsilon_{11}^S/\varepsilon_0$	$\varepsilon_{33}^S/\varepsilon_0$	e_{15}	e_{31}	e_{33}
14.7	9.37	11.3	2.30	1130	914	11.64	-3.09	16

The plate is assumed to be infinite along *x2* axis, its thickness Th is along *x3* while its length L is along *x1*. It has a length-to-thickness ratio (L/Th) of approximately 14 which is around a minimum to keep the thickness mode predominant. All losses are considered negligible compared to the mechanical ones. The piezoelectric element is immersed in water and the configuration of the simulation is detailed in Table 2.

Table 2. Configuration used for the simulation of the piezoelectric plate immersed in water.

e_p	L/Th	ρ	α	c_l	f_e	λ_p
43.3	14	7700	0.085	4335	50	86.7

e_p (μm): thickness of the piezoelectric bar; L/Th: length-to-thickness ratio; ρ (kg/m^3): density; α ($dB/mm/MHz$): acoustic attenuation; c_l (m/s): longitudinal wave velocity; f_e (MHz): excitation frequency; λ_p (μm): acoustic wavelength in the piezoelectric material.

To observe and compare the results of the simulations using FD-PSTD and FE algorithms, the pressure field is picked up at a fluid node (above the top electrode) just in front of the middle of the piezoelectric plate, and its evolution is presented on Fig. 2.

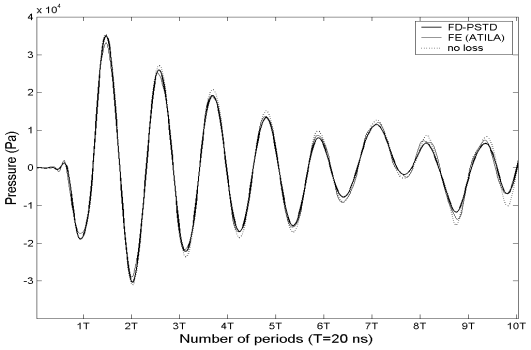

Fig.2. Evolution of the pressure in water in front of the piezoelectric plate, on the central axis, simulated using FD-PSTD and FE methods. These results are compared to the lossless case (FD-PSTD).

As expected, the mechanical losses slightly attenuates the oscillations of the pressure field, and the result of the FD-PSTD method is in good agreement with the one obtained using ATILA® software. The simulation lasts long enough to observe the perturbation introduced by the incoming transversal waves, but the acoustic response for this simple configuration is very long. The use of a backing and of a front matching layer produces a much shorter response.

C.2. Transducer configuration

In order to simulate the acoustic waves generated by a piezoelectric element in the configuration of a real transducer, we add a backing and a matching layer on the faces of the active element. The characteristics of this piezoelectric element were previously described in Table 1. The configuration used is illustrated on Fig. 3 and the characteristics of the materials are summed up in Table 3.

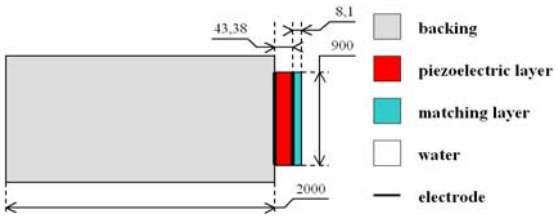

Fig.3. Simulated configuration of the transducer (dimensions are given in µm).

The L/Th ratio of the piezoelectric element is now 20 to emphasize the thickness mode. The acoustic impedance was imposed at 6 MRa. Thus, using an homogenization model [9] and considering an epoxy resin loaded with tungsten powder, a volume fraction of 15% of metallic powder is necessary. The longitudinal wave velocity is then deduced with this model (Table 3). With the KLM scheme and an optimization algorithm, the thickness and the acoustical impedance of the front matching layer were calculated. Values are summarized in Fig. 3 and Table 3. This optimization was performed for medical imaging applications and corresponds to a trade-off between sensitivity and bandwidth of the electro-acoustic response of the transducer.

doi:10.3728/ICUltrasonics.2007.Vienna.1227_filoux

Table 3. Characteristics of the materials used for the transducer components.

Component	Thickness (μm)	ρ (kg/m^3)	c_l (m/s)	c_t (m/s)	Z (MRa)	α $(dB/mm/MHz)$
Piezoelectric layer	43.3	7700	4335	2530	33.4	0.085
Backing	2000	3830	1575	780	6	0.48
Matching layer	8.1	4490	1530	765	6.9	0.50

The propagation over time of the acoustic waves inside the structure of the transducer can be observed in Fig. 4. The study is focused on the waves propagating in the close space surrounding the piezoelectric layer. Fig. 4a) is a snapshot taken at t=10 ns (0,5T) on which we can see the stress field created inside the piezoelectric media by the electrical excitation (T=20 ns). The acoustic waves then propagate in the backing above and in the front matching layer below. On Fig. 4b), taken at t=60 ns (3T), the waves have spread into water and they are absorbed by the PMLs at the borders of the computational space.

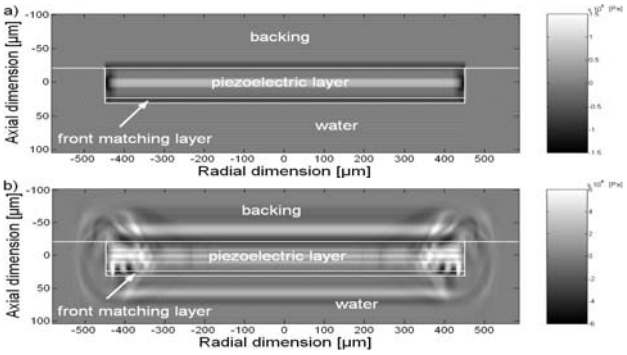

Fig.4. Stress field and pressure in the computational domain at instants a) t=10 ns (T/2) and b) t=60 ns (3T). The temporal period T corresponds to the central frequency of the transducer.

To compare these results with those of ATILA® software, we pick up the the pressure in water on the central axis of the transducer, a few µm in front of the matching layer. The results are obtained by the PS-FDTD and the FE method using a meshing of λ/12 width square cells, with λ=30µm the acoustic wavelength in water. As the modeling of PMLs is not enabled in the FE algorithm used, the time-processing required by the FD-PSTD method is around a thousand times shorter than that of the FE software. The results are presented in Fig. 5.

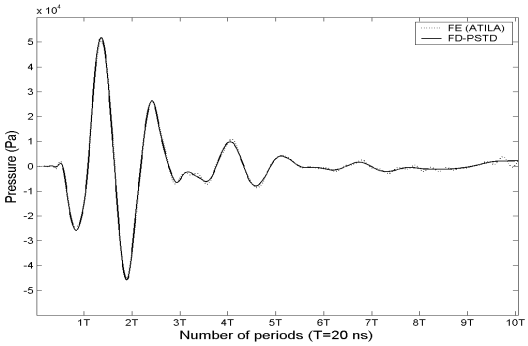

Fig.5. Evolution of the pressure in water in front of the matching layer, on the central axis of the transducer, simulated using FD-PSTD and FE methods.

They are similar to the usual response of a transducer with this configuration. The extra oscillations obtained with the FE method are typically due to the fact that it requires a more accurate meshing than the FD-PSTD method to provide exact solutions.

D. Conclusion

A new hybrid FD-PSTD algorithm has been developed to model a piezoelectric resonator in various configurations. Its purpose is to keep the advantage of the PSTD method to efficiently simulate the propagation of acoustic waves over the large structures of a transducer, and the advantage of the FDTD method to model resonators with various geometries and materials. The presented results are obtained with the simulation of transducers with simple configurations, but they are in good agreement with those of ATILA® software and they validate the efficiency of the FD-PSTD algorithm.

The future work will be the extension of the algorithm to axisymmetrical geometry so as to enable the modeling of piezoelectric disk resonators, excited by various electrical conditions.

E. Acknowledgements

Work performed in the frame of MIND FP6 network of excellence (contract no. 515757_2). The authors thank D. Certon and O. Bou Matar for their help on the model determination.

F. Literature

[1] Fornberg B., "The pseudospectral method : Comparisons with finite differences for the elastic wave equation", Geophysics 52, 483-501, 1987.

[2] Liu Q.H., "The PSTD algorithm: A time-domain method requiring only two cells per wavelength", Microwave Opt. Tech. Lett., 158-165, 1997.

[3] Yuan X *et al.*, "Formulation and validation of Berenger's PML absorbing boundary for the FDTD simulation acoustic scattering", IEEE Trans. Ultrason. Ferroelect. Freq. Contr. 44, 816-822, 1997.

[4] Chagla F., Smith P.M., "Finite difference time domain methods for piezoelectric crystals", IEEE Trans. Ultrason. Ferroelect. Freq. Contr. 53, 1895-1901, 2006.

[5] Dubus B *et al.*, "Analysis of mechanical limitations of high power piezoelectric transducers using finite element modelling", Ultrasonics 29, 201-207, 1991.

[6] Auld B.A., "Acoustic Fields and Waves in Solids", Wiley, New-York, 1990.

[7] Ghrist M *et al.*, "Staggered time integrators for wave equations", SIAM J. Numer. Anal. 38 (3), 718-741, 2000.

[8] Fornberg B., Sloan D.M., "A review of pseudospectral methods for solving partial differential equations", Acta Numerica, 203-267, 1994.

[9] T. Nguyen *et al.*, "Experimental verification of the theory of elastic properties using scattering approximations in (0-3) connectivity composite materials", IEEE UFFC 43(4), 640-645, 1996.